

Targeting Colorectal Cancer with Conjugates of a Glucose Transporter Inhibitor and 5-Fluorouracil

Chun-Kai Chang, Pei-Fang Chiu, Hui-Yi Yang, Yu-Pu Juang, Yen-Hsun Lai, Tzung-Sheng Lin, Lih-Ching Hsu, Linda Chia-Hui Yu, and Pi-Hui Liang*

Cite This: *J. Med. Chem.* 2021, 64, 4450–4461

Read Online

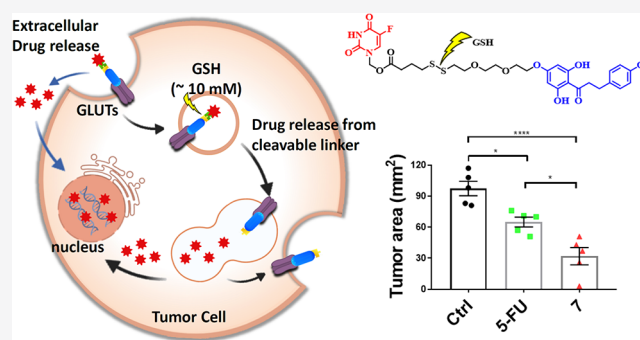
ACCESS |

Metrics & More

Article Recommendations

Supporting Information

ABSTRACT: Overexpression of glucose transporters (GLUTs) in colorectal cancer cells is associated with 5-fluorouracil (1, 5-FU) resistance and poor clinical outcomes. We designed and synthesized a novel GLUT-targeting drug conjugate, triggered by glutathione in the tumor microenvironment, that releases 5-FU and GLUTs inhibitor (phlorizin (2) and phloretin (3)). Using an orthotopic colorectal cancer mice model, we showed that the conjugate exhibited better antitumor efficacy than 5-FU, with much lower exposure of 5-FU during treatment and without significant side effects. Our study establishes a GLUT-targeting theranostic incorporating a disulfide linker between the targeting module and cytotoxic payload as a potential antitumor therapy.



INTRODUCTION

Colorectal cancer (CRC) is the fourth most common and second most lethal cancer in the world, with 19.7 million cases and almost 880,000 deaths in 2018.¹ First line chemotherapy consists of 5-fluorouracil (1, 5-FU), in combination with other reagents such as FOLFOX4 (leucovorin, 5-FU, and oxaliplatin), FOLFIRI (leucovorin, 5-FU, and irinotecan), and FOLFOXIRI (5-FU, leucovorin, oxaliplatin, and irinotecan).^{2–4} The 5-FU-based chemotherapy is efficacious in patients with metastatic CRC but poorly selective for malignant vs healthy cells, causing marrow suppression and polyneuropathy, both major dose-limiting toxicities.⁵ Chemotherapy resistance is also a significant problem and the main reason for the high mortality rate of CRC.²

Cancer cells rely on anaerobic glycolysis pathways to a greater extent than mitochondrial oxidative phosphorylation compared to noncancer cells, the so-called Warburg effect.⁶ There are two categories of glucose transporters that enable cancer cells to uptake glucose: (1) facilitative GLUT1 to GLUT4,^{7,8} and (2) secondary active sodium-glucose cotransporters (SGLT-1 and SGLT-2).^{9,10} Tumor cells also overexpress glycolysis enzymes and glucose transporters, both of which were correlated with the invasiveness and metastatic potential of cancers,^{11–14} and enhanced glucose uptake is known to diminish the cytotoxicity of 5-FU in colorectal cancer.^{15,16} We analyzed specimens from CRC patients previously treated with 5-FU and found significantly higher transcript levels of SGLT-1 and GLUT1 in those refractory to the therapy.¹⁷ Overexpression of GLUTs is known to be associated with 5-FU resistance in colon cancer

cells through pyruvate scavenging of free radicals involved in 5-FU-induced cytotoxicity.¹⁷

Targeting of glucose transporters has attracted a great deal of interest as an anticancer strategy in recent years.^{18,19} Phloretin (3, Figure 1), a well-known and naturally abundant GLUT1 inhibitor, has been investigated for its anticancer activities and demonstrated the ability to overcome therapeutic resistance of anticancer agents when administered in combination with them in preclinical studies.^{20–23} Phlorizin (2, Figure 1) is a SGLT-1 inhibitor that differs from phloretin in that it bears an additional glucose conjugate at the *ortho*-hydroxyl of a phenyl moiety. Treatment of mice bearing tumor xenografts with SGLT inhibitors resulted in increased necrosis within the tumors.²⁴ Since these glucose transporters are physiologically expressed in a wide array of cells and tissues,^{25–27} selective targeting of SGLT-1 or GLUT1 on cancer cells would be necessary. One possible approach is through a small molecule drug conjugation (SMDC) strategy,^{28,29} but to the best of our knowledge, SMDC using glucose transporter inhibitors as a targeting ligand has not been attempted.

Such a strategy is predicated on the ability to selectively release the conjugated drug in the tumor tissue. Given that the concentration of GSH is about 10-fold higher in tumor cells

Received: May 27, 2020

Published: April 5, 2021



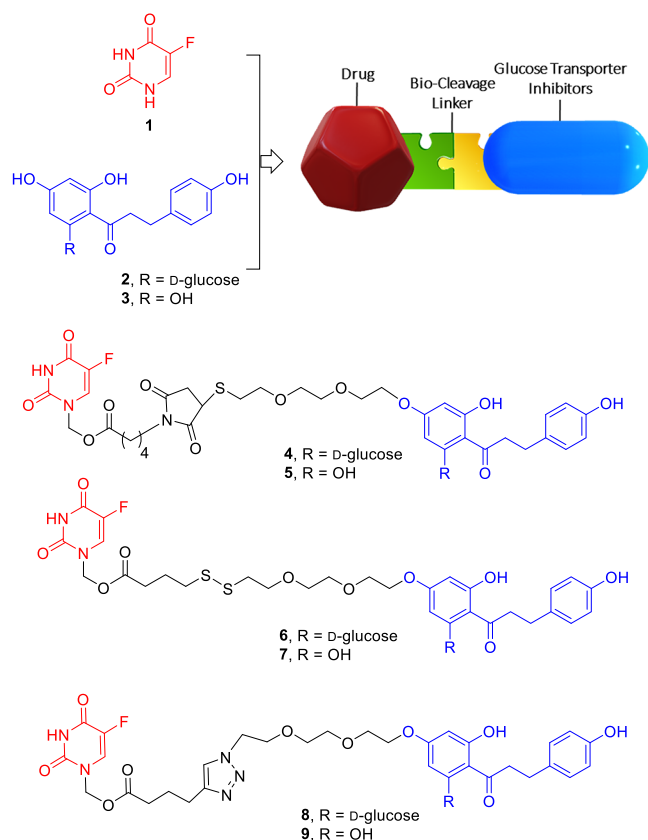


Figure 1. Structures of 5-FU (1), phlorizin (2), and phloretin (3) and proposed design of glucose transporter-targeting drug conjugates 4–9.

compared to the normal cells (except hepatocytes) and 10–100 times higher intracellularly,^{30–32} we designed compounds 4–7, wherein phloretin 3 (or phlorizin 2) are connected to 5-FU through a redox-sensitive linker, as depicted in Figure 1. In conjugates 4 and 5, a succinimidyl thioether (a moderately sensitive linker)³³ was used, whereas conjugates 6 and 7 incorporate a disulfide linker (a highly sensitive linker) instead. We also designed compounds 8 and 9, incorporating triazole conjugates as a stable linker-bearing group (Figure 1). The stability of these conjugates in human plasma and in solutions containing varying concentrations of GSH was studied as well as their *in vitro* cytotoxicity across two tumor cell lines (HCT-116 and HT-29). The antitumor effect of the compounds was evaluated in the orthotopic CRC mice model, and pharmacokinetic evaluation was performed to elucidate tumor-targeting efficacy.

RESULTS AND DISCUSSION

Chemistry. Conjugates 4–9 were constructed by sequential derivatization of the central linker (Scheme 1, detailed synthesis procedures can be found in the Supporting Information). Addition of triethylene glycol and TsCl to ethanol/H₂O gave the tosylated intermediate, to which was added potassium thioacetate in acetone. After this mixture was heated at reflux for 1 h, thiol ester 11 was obtained in 85% yield. Hydrolysis of thiol ester 11 was accomplished using potassium carbonate (0.05 M) to give compound 12 in 85% yield, the free thiol of which was protected using 2-methyl-2-propanethiol to give compound 13 in 70% yield. After mesylation and bromide substitution, brominated compound 14 was obtained in 57% yield. Alkylation of phlorizin with 14 using potassium carbonate

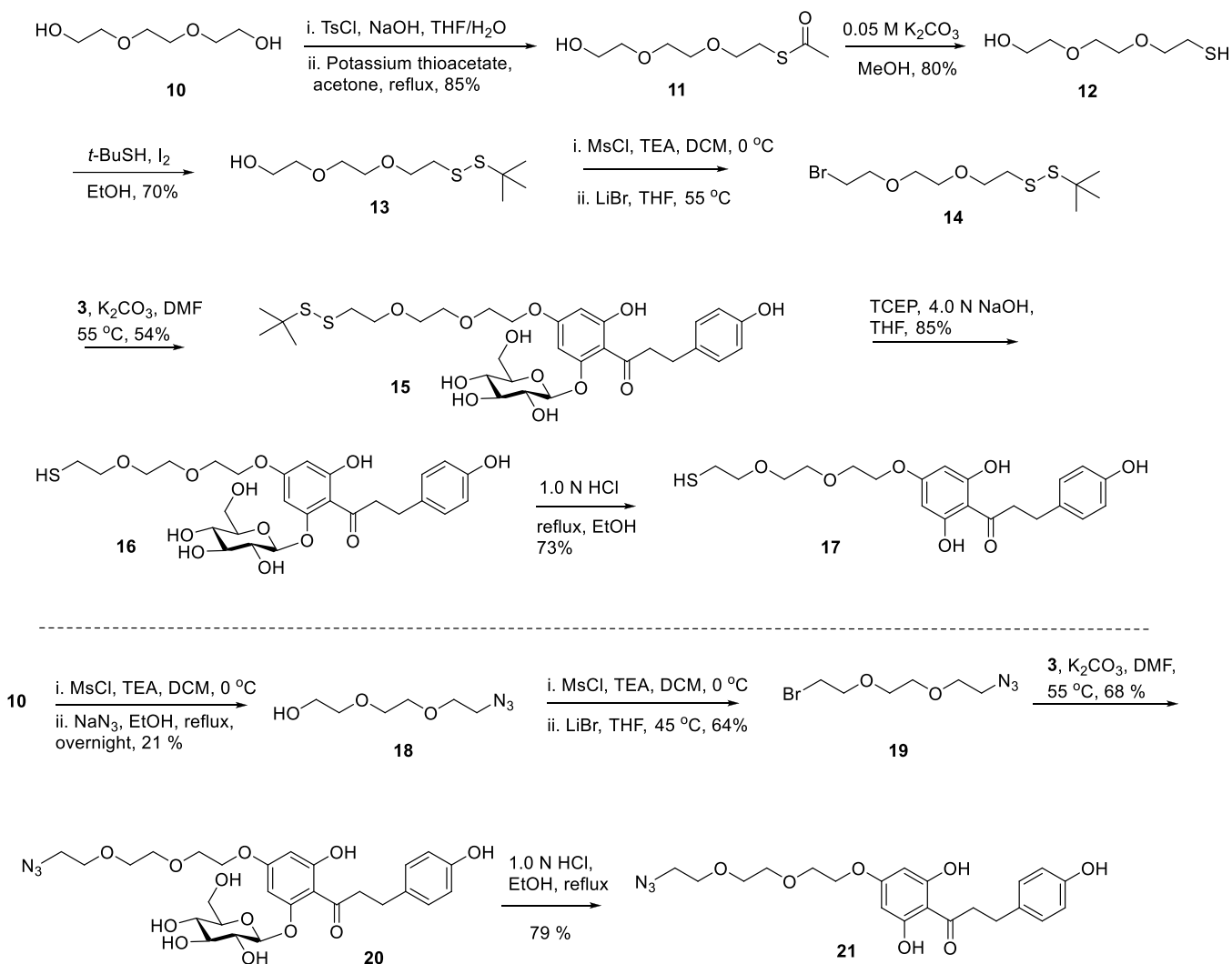
as a base gave compound 15 (54%) as a major product. The regioselective nature of this alkylation was presumably due to the electro-withdrawing effect of the carbonyl group at the *para*-position of a benzyl group and the reduced steric hindrance at this position. Deprotection of a *t*-butylthiol group by 4.0 N NaOH and TCEP gave phlorizin derivative 16 in 85% yield, which was refluxed with 1.0 N HCl at 90 °C for 3 h quenching with NaHCO₃(aq) to give phloretin derivative 17 (73% yield).

Phlorizin- and phloretin azide-containing analogs 20 and 21 were similarly prepared. MsCl was added slowly to a solution of triethylene glycol and triethylamine in DCM at 0 °C, with stirring. After 20 min, the reaction mixture was concentrated and the residue was dissolved in EtOH, to which was added NaN₃. After refluxing for 24 h, azide linker 18 was obtained. This was mesylated, and then the mesyl group exchanged with bromine using lithium bromide to provide compound 19, which was used to derivatize phlorizin to give the desired intermediate 20. After hydrolysis, phloretin derivative 21 was obtained.

N-1 alkyl-substituted 5-FU derivatives are poorly cytotoxic and not converted to 5-FU *in vivo*.³⁴ In anticipation of this problem, ester functionality was designed into the linker; it was hypothesized that this ester would be cleavable in the tumor microenvironment by endogenous esterases. The reaction of 5-FU with formaldehyde followed by 6-maleimidohexanoic acid, 4-(pyridin-2-ylsulfanyl)-butanoic acid, or 4-pentynoic acid and the coupling reagents DCC and DMAP gave compounds 22–24, respectively (Scheme 2). Thiol-containing phlorizin derivative 16 and phloretin derivative 17 were conjugated with maleimide of 5-FU (22) to give 4 and 5, respectively, and the carboxylic acid of 23 to give 6 and 7, respectively. Azide-containing phlorizin derivative 20 and phloretin derivative 21 were conjugated with alkyne-containing 5-FU (24) under the (Cu(I)-catalyzed azide-alkyne cycloaddition) click condition to give compounds 8 and 9.

Plasma Stability and Release Profiles in Different GSH Concentrations. The *in vitro* human plasma stability and release profiles of compounds 5, 7, and 9 are depicted in Figure 2. The stability tests comprised incubation of compounds 5, 7, and 9 in human plasma at 37 °C at different time intervals 0, 1, 2, 4, 8, 12, 24, and 48 h. Samples were collected and analyzed by RP-HPLC (Figure 2a for 7 and Figure S49 for 5 and 9). As shown in Figure 2b, the half-lives of compounds 5, 7, and 9 were 0.8, 13, and 3.6 h, respectively. The reason for the inferior plasma stability of compounds 5 and 9 compared to 7 is unknown but can be attributed to the high pK_a of the linkers (the pK_a values of both succinimide and triazole are around 8.5–9.5) increasing the susceptibility of the ester portion of the linker to degradation.³⁵ Therefore, pH stability analysis of compound 9 was conducted, and it was found that compound 9 was stable at pH 4–5 but was prone to fully degrade when the pH was ≥7. In order to predict the fate of those conjugates in the body, we collected the metabolites of 7 from the plasma treating assay and identified two major metabolites: metabolite 1, which arises from hydrolysis of the ester bond of 7, and metabolite 2, the disulfide exchange intermediate (Figure 2a and Figure S48). Since the concentration of GSH is about 5–10 mM in the tumor cells and 1–10 μM in plasma,³⁶ we then evaluated the release of 5-FU from conjugates 5, 7, and 9 using GSH. The concentration of GSH used was set to 5 mM, mimicking the tumor microenvironment. Less 5-FU was released from compounds 5 and 9 after 48 h; however, the release of 5-FU from compound 7 was found to be dependent on the concentration of GSH used. The cleavage percentage of compound 7 after 4 h exposure to 5

Scheme 1. Synthetic Route for Phlorizin and Phloretin Conjugates



mM GSH was up to 60% but only ~10% in the presence of 1 mM GSH, indicating that compound 7 is cleaved much slower in 1 mM GSH than 5 mM GSH (Figure 2d). The half-lives of compound 7 at 5 and 1 mM GSH were 4.0 and 10.3 h, respectively. In the presence of 5 μM GSH, only 30% degradation of compound 7 was observed after 48 h (Figure 2d). The stability and release profiles of three phlorizin-bearing derivatives 4, 6, and 8 were also evaluated; their results were all similar to their corresponding congeners 5, 7, and 9, respectively. Disulfide bonds in compounds 6 and 7 have relatively short half-lives (<5 h) in highly reductive environments while maintaining a degree of stability in circulation.

GLUT1 Inhibitory Activity. A previous crystallography study established that the benzene-1,3,5-triol ring of phloretin is stabilized in a pocket of GLUT1 by forming three H-bonds,³⁷ but the extent to which this would be perturbed by a substituent at the 4-position (such as in our phloretin derivatives 17) was unknown. We examined the inhibitory activity of 16 and 17 toward GLUT1 using COS-7 cells that overexpress GLUT1 in a 2-NBDG ((2-*N*-(7-nitrobenz-2-oxa-1,3-diazol-4-yl)amino)-2-deoxy-D-glucose) uptake assay.²² Since phlorizin could not inhibit GLUT1, it was not surprising that compound 16 (a phlorizin derivative) was not able to inhibit GLUT1 at either 50 or 100 μM (Figure 3). On the contrary, compound 17 had

similar inhibition activity to phloretin, despite bearing substitution at 4-OH.

Cytotoxicity to Human CRC Cells. Compounds 4–9, 16–17, and 5-FU were evaluated for their cytotoxicity against the CRC cell lines HCT-116 and HT-29 (both of which overexpress GLUT1, Figure S50) using the sulforhodamine B (SRB) assay (Table 1).^{38–40} 5-FU exhibited an IC_{50} of approximately 15 μM in CRC cells (entry 1, Table 1). To mimic the tumor microenvironment, 10 mM GSH was first attempted to add to the medium;⁴¹ however, we found that 10 mM GSH interfered CRC cell growth. Thus, 5 mM GSH was added to the culture media of CRC cell lines. Phlorizin derivative 16 did not exhibit any inhibitory activity. Derivative 17 exhibited some inhibitory activity, with an IC_{50} of 15–30 μM . Derivatives 4 and 5 were poorly cytotoxic, with or without the addition of GSH. The cytotoxicity of the disulfide-containing compounds 6 and 7 was sensitive to GSH, for example, the IC_{50} of 6 to HCT-116 cells was 23.8 μM with GSH and 54.9 μM without GSH. These cytotoxicities of 6 and 7 in these cancer cells might be due to the sub-millimolar level of intracellular GSH that gradually cleaved the disulfide bonds of 6 and 7 to release 5-FU. The IC_{50} of 7 in the presence of GSH was 10.5 μM for HCT-116 and 3.8 μM for HT-29, which were close to the IC_{50} values of 5-FU in both cell lines (13.9 and 5.2 μM , respectively). Compounds 8 and 9 were

Scheme 2. Synthetic Route for the Conjugates 4–9

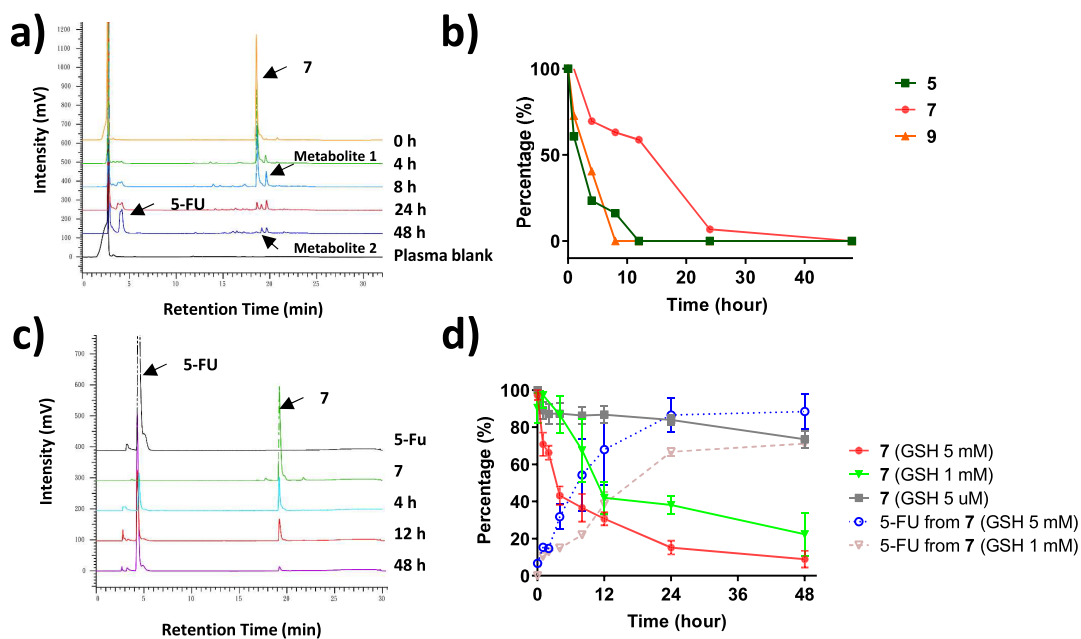
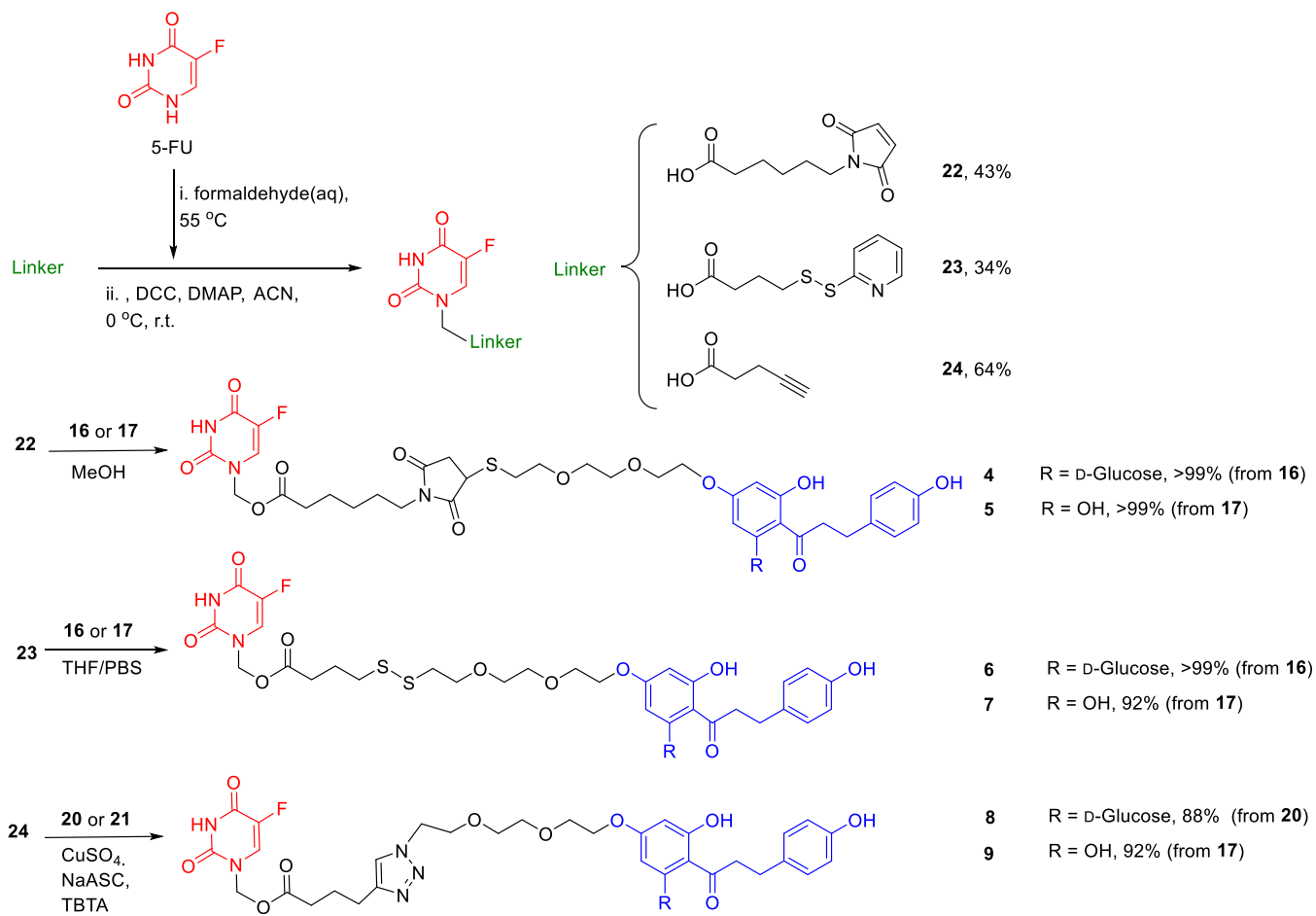


Figure 2. *In vitro* plasma stability and release profiles of compounds under different conditions. (a) Analysis of compound 7 with human plasma by using RP-HPLC. (b) Stability of compounds 5, 7, and 9 in human plasma at 37 °C. (c) Analysis of compound 7 with GSH (5 mM) by using RP-HPLC. (d) *In vitro* release profile of compound 7 under different GSH concentrations (5 μM, 1 mM, and 5 mM) and formations of 5-FU under 1 and 5 mM GSH. Data are shown as mean ± S.E.M. ($n = 3$).

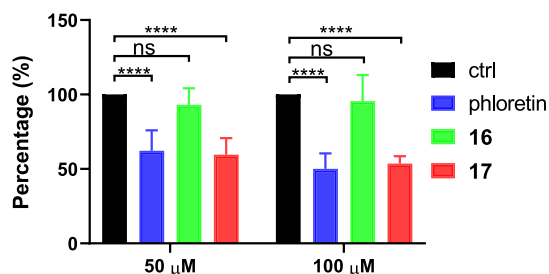


Figure 3. Inhibition of GLUT1 activity of compounds 16 and 17 by the 2-NBDG uptake assay. Data represent mean \pm S.E.M. ($n = 4$; n.s., nonsignificant difference; **** $P < 0.0001$ (two-way ANOVA)).

Table 1. Cytotoxicity of Compounds 4–9, 16–17, and 5-FU in HCT-116 and HT-29 Cell Lines^a

compounds	HCT-116 (μM)		HT-29 (μM)	
	w/o GSH	5 mM GSH	w/o GSH	5 mM GSH
5-FU	14.9 \pm 2.24	13.9 \pm 0.60	14.9 \pm 1.86	5.20 \pm 0.12
16	>100	>100	>100	>100
17	15.5 \pm 0.72	15.9 \pm 0.89	29.1 \pm 6.14	24.2 \pm 0.40
4	97.4 \pm 20.3	>100	>100	93.6 \pm 9.4
5	75.0 \pm 13.7	82.8 \pm 4.18	43.7 \pm 5.0	86.9 \pm 2.9
6	54.9 \pm 3.36	23.8 \pm 1.15	59.8 \pm 7.93	8.00 \pm 0.52
7	21.2 \pm 1.69	10.5 \pm 1.15	19.6 \pm 3.86	3.80 \pm 0.65
8	>100	ND ^b	>100	ND ^b
9	>100	ND ^b	85 \pm 9.1	ND ^b
5-FU + 16	21.9 \pm 2.98	13.6 \pm 0.73	21.0 \pm 9.38	8.58 \pm 0.09
5-FU + 17	10.4 \pm 1.25	8.73 \pm 0.64	10.3 \pm 4.33	3.03 \pm 0.03

^aCell lines were incubated with compounds for 48 h. IC₅₀ values were determined by SRB assay. ^bND = not determined.

poorly cytotoxic. The cytotoxicities of 16 and 17 were also assayed in combination with 5-FU: 5-FU combined with 17 was more effective at inhibiting cell viability than the other compounds when given alone, reflecting a synergistic inhibitory effect. Additionally, the cytotoxicities of 5-FU and 7 in the low expression GLUT1 normal cell line NHDF (western blot analysis of GLUT1 in Figure S50) were also examined; it was

found that both 5-FU and 7 had no obvious inhibition effect (IC₅₀ values of 70.4 \pm 7.2 and 90.0 \pm 2.6 μM , respectively), suggesting that the conjugate 7 was less toxic in normal cells.

Evaluation of the *In Vivo* Activity of the Synthetic Compounds in an Orthotopic CRC Mice Model. Compound 7 was selected for *in vivo* evaluation based on its release profile and the results of the cytotoxicity experiments. An orthotopic CRC mice model was established by intraperitoneal (i.p.) injection of AOM (10 mg/kg body weight) to BALB/c mice (6 weeks, male) and supplementation of their drinking water with 2% dextran sodium sulfate (DSS) (Figure 4a).^{39,42} After 2 months, solutions of 5-FU (50 mg/kg), compound 7 (50 mg/kg), and 5-FU + 17 (10 mg/kg of 5-FU and 30 mg/kg of 17, dosing is based on compound 7) in 0.2 mL of PBS were injected i.p. once every 3 days for 3 weeks. Based on calculations of tumor volume, compound 7 showed better tumor suppression than 5-FU at a dose of 50 mg/kg (0.07 mmol, when only 19% of 5-FU was given (Figure 4b,c)). Since GLUT1/3/4 is generally overexpressed in CRC patients¹⁷ and phloretin is known to inhibit GLUT1/3/4 inhibition,^{43,44} compound 7 might display targeting through GLUT1/3/4, leading to significant tumor inhibition. Mice treated with free 5-FU were noted to lose about 10% of their body weight rapidly after injection (Figure 4d), presumably a reflection of the systemic toxicity of 5-FU; there was no significant change in the body weight of the mice who received compound 7. The combination of 5-FU (with 19% of free 5-FU dose) and compound 17 also reduced tumor size in the mice model, exhibiting synergistic effects, which was also observed in the cell assay.

Evaluation of Pharmacokinetic and Biodistribution Profiles. Plasma concentration and organ distribution of compound 7 were evaluated in BALB/c mice ($n = 3$) with single dose injection of compounds. To analyze the 5-FU release profile of compound 7, blood samples were collected at 1, 3, 5, 10, 15, 30, and 45 min and 1, 2, 4, and 8 h after intravenous injection (i.v.) (50 mg/kg), and the concentration of compound 7 was determined with UPLC-MS/MS. The concentration of compound 7 dropped rapidly in 10 min (Figure 5a), presumably related to the expression of carboxylesterase and dihydropyrimidine dehydrogenase (DPD) and the high tissue penetration

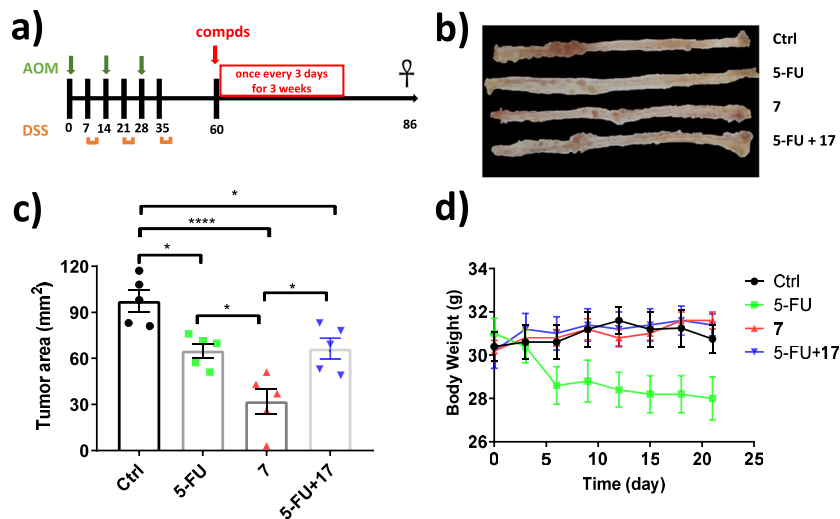


Figure 4. (a) Schematics of the mouse model for CRC. (b) Macroscopic pictures of the mice colonic tumors. (c) Tumor area and (d) body weight change of the mice treated with control (PBS alone), 5-FU (50 mg/kg), 7 (50 mg/kg), and 5-FU + 17 (10 mg/kg of 5-FU and 30 mg/kg of 17, dosing is based on compound 7). Data represent mean \pm S.E.M. ($n = 5$, **** $P < 0.0001$ or * $P < 0.05$ (one-way ANOVA)).

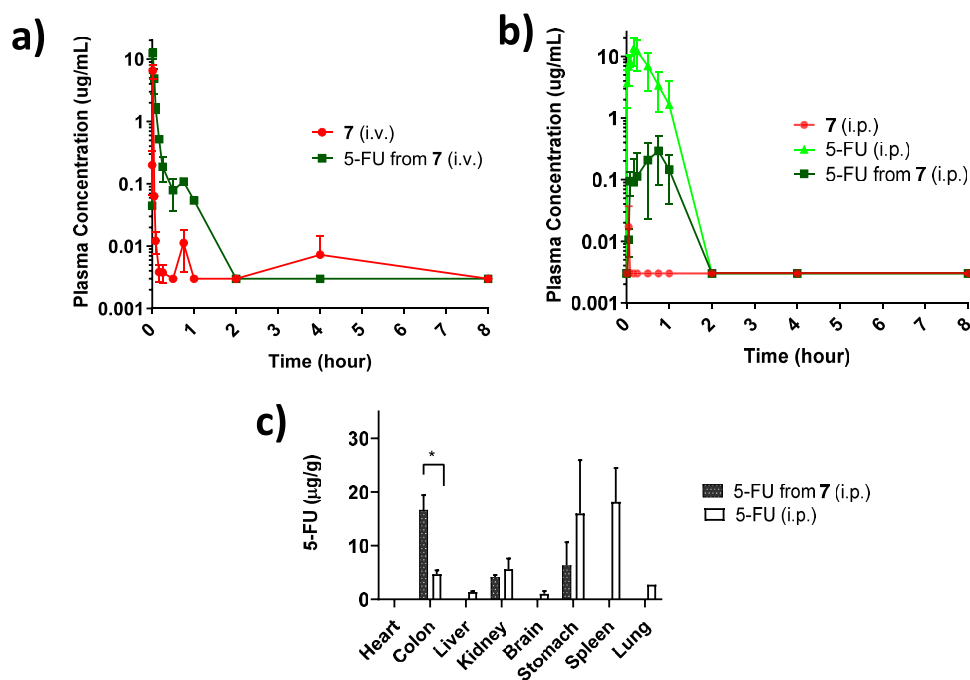


Figure 5. Pharmacokinetic profile of compound 7 and 5-FU in mice following i.v. and i.p. injection. (a, b) Plot shows plasma concentration as the function of time after i.v. injection of compound 7 (50 mg/kg) and i.p. injection of compound 7 and 5-FU (50 mg/kg). The data points exhibiting concentrations lower than the detection limit of the LC–MS/MS method used were arbitrarily placed just below 0.003 $\mu\text{g}/\text{mL}$. (c) Distributions of 5-FU at 1 h after i.p. injection of free 5-FU (9.5 mg/kg) and compound 7 (50 mg/kg, 5-FU equivalent dose) in BALB/c mice. Data represent mean \pm S.E.M. ($n = 3$, $*P < 0.05$).

of 7 in mouse blood.^{43–45} 5-FU released from compound 7 was detected within 2 h and persisted in blood longer than compound 7 (Figure 5a). Compound 7 exhibited an unusual plasma pharmacokinetic (PK) profile in that its concentration was undetectable (lower detection limit = 0.003 $\mu\text{g}/\text{mL}$) after 30 min but detectable again after 45 min and 4 h, suggesting it to be rapidly absorbed by mouse cells and tissues and reach an equilibrium during elimination.⁴⁶ To investigate the distribution-related antitumor efficacy of compound 7, blood samples were collected after intraperitoneal injection (i.p.) (50 mg/kg) of compound 7 and 5-FU in BALB/c mice ($n = 3$). The concentration of compound 7 was below the detection limit after 5 min due to lipophilicity-directed high tissue penetration.⁴⁷ The T_{max} of 5-FU from compound 7 was delayed from 10 to 45 min compared to the 5-FU group, and the concentration of 5-FU in both groups was undetectable after 2 h, indicating that the antitumor efficacy might be related to high tissue penetration (Figure 5b). Consequently, the distributions of compound 7 (50 mg/kg, 5-FU equivalent dose) and 5-FU (9.5 mg/kg) in the organs of BALB/c mice were evaluated at 1 h post i.p. injection; compound 7 was found to be distributed in the stomach, colon, heart, and liver (Figure S56). Since the amounts of compound 7 in each organ were low, further analysis of 5-FU released from compound 7 was performed, showing that 5-FU was detected mainly in colon, with small amounts in the kidney and stomach, while free 5-FU was distributed in stomach, spleen, and kidney (Figure 5c), similar to the previous report.⁴⁸ These results indicate that our conjugation of compound 7 is an appropriate strategy to effect the delivery of 5-FU into the colon. This delivery is posited to be mediated by GLUT1, which is mostly expressed in the colon. As the phloretin moiety binds to the glucose transporter, two pathways by which cleavage of the disulfide bond might be accomplished: extracellularly, after binding of GLUT, or intracellularly, after the conjugate

distributes to the cytosol of CRC cell, where GSH is 10-fold more than the normal cells. The high tissue penetration of 7 led to the delayed release of 5-FU, prolonging exposure to 5-FU and enhancing its tumor eradicating effects. Organ distribution analysis revealed the colon-targeting effect of 5-FU, leading to promising antitumor efficacy with low toxicity.

CONCLUSIONS

A series of drug conjugates comprising 5-FU and either phlorizin or phloretin joined with a succinimidyl thioether, disulfide, or triazole linker have been designed, synthesized, and biologically evaluated. Most of these compounds were less potent against CRC cell lines than 5-FU; however, compound 7, incorporating 5-FU, phloretin, and a disulfide bond, showed good stability ($t_{1/2} = 13$ h) in human plasma and lability in the presence of 5 mM GSH ($t_{1/2} = 4.0$ h), and its cytotoxicity toward HCT-116 and HT-29 cell lines was similar to that of 5-FU. In an orthotopic mice CRC model, compound 7 exhibited excellent antitumor efficacy and low toxicity, reducing tumor volume by 67% (only a 33% reduction was seen with 5-FU) without body weight loss. The colon-targeting effect was a consequence of high tissue penetration and GLUT-targeting efficacy, leading to considerable tumor inhibition in comparison to 5-FU. Targeting GLUT with cytotoxic small molecule drugs conjugated with the glutathione-sensitive linker is therefore proposed as a novel strategy for the treatment of CRC. Further work to expand this conjugation strategy to other anticancer agents with a view to the development of novel chemotherapeutic agents in the future is ongoing in our laboratory.

EXPERIMENTAL SECTION

General Chemicals. Reagents and solvents for synthesis were of reagent grade and used without further purification. HPLC analysis was performed on a HITACHI D-2000 Elite system equipped with a BDS

HYPERSIL C18 250-4.6 column. The mobile phase was a mixture of ACN and dd H₂O, which were filtered through a 0.45 mm membrane filter before use. The column was eluted with the mobile phase at a flow rate of 1.0 mL/min. The eluate was monitored by measuring the absorption at 254 nm at 25 °C. The purities of all final products were confirmed by HPLC to be >95% prior to their *in vitro* and *in vivo* use. Thin-layer chromatography (0.25 mm, E. Merck silica gel 60 F₂₅₄) was used to monitor reaction progress; plates were visualized by UV (254 nm) or by staining with ninhydrin and heating. Acquisition of ¹H and ¹³C nuclear magnetic resonance (NMR) spectra was performed on a Bruker-AV-400 (400 MHz) (See the Supporting Information). Chemical shifts are referenced to residual solvent peaks in parts per million (δ): ¹H δ = 2.50, ¹³C δ = 39.52 for *d*₆-DMSO; ¹H δ = 3.31, ¹³C δ = 49.00 for CD₃OD; ¹H δ = 2.05, ¹³C δ = 29.84, 206.26 for *d*₆-acetone; ¹H δ = 7.26, ¹³C δ = 77.16 for CDCl₃. Coupling constants (*J*) are given in Hertz (Hz). Splitting patterns are denoted as s (singlet), d (doublet), dd (double doublet), t (triplet), q (quartet), and m (multiplet). Mass spectra were acquired using a Bruker bioTOF III and are reported in *m/z*.

(5-Fluoro-2,4-dioxo-3,4-dihydropyrimidin-1(2H)-yl)methyl 6-((2-(2-(2-(3-hydroxy-4-(3-(4-hydroxyphenyl)propanoyl)-5-(((2S,3R,5S,6R)-3,4,5-trihydroxy-6-(hydroxymethyl)-tetrahydro-2H-pyran-2-yl)oxy)phenoxy)ethoxy)ethoxy)ethyl)-thio)-2,5-dioxopyrrolidin-1-yl)hexanoate (4). To a solution of 16 (35 mg, 0.06 mmol) in dry methanol (2 mL) was added compound 22 (21 mg, 0.06 mmol). The reaction mixture was stirred for 10 min and then was concentrated *in vacuo*. The residue was purified by column chromatography (silica gel; DCM/MeOH = 12/1) to give 4 (53 mg, 0.06 mmol, >99%) as foam. ¹H NMR (600 MHz, CD₃OD) δ 7.88 (d, *J* = 6 Hz, 1H, H-29), 7.07 (d, *J* = 8.2 Hz, 2H, H-2, H-6), 6.67 (d, *J* = 8.2 Hz, 2H, H-3, H-5), 6.31–6.29 (m, 1H, H-3'), 6.11–6.09 (m, 1H, H-5'), 5.61 (s, 2H, H-23), 5.11 (d, *J* = 7.2 Hz, 1H, H-1''), 4.15 (t, *J* = 4.8 Hz, 2H), 4.03–4.00 (m, 1H), 3.90 (d, *J* = 4.2 Hz, 1H), 3.81 (t, *J* = 4.2 Hz, 2H), 3.77–3.70 (m, 3H), 3.67 (t, *J* = 4.2 Hz, 2H), 3.63 (t, *J* = 5.4 Hz, 2H), 3.50–3.45 (m, 5H), 3.42–3.30 (m, 3H), 3.17–3.11 (m, 1H), 3.09–3.05 (m, 1H), 2.89–2.81 (m, 3H), 2.50 (dd, *J*₁ = 15.6, 3 Hz, 1H), 2.33 (t, *J* = 7.2 Hz, 2H, H-21), 1.60–1.58 (m, 2H, H-20), 1.52–1.50 (m, 2H, H-18), 1.28–1.26 (m, 2H, H-19) ppm; ¹³C NMR (150 MHz, CD₃OD) 206.8, 178.9, 177.2, 174.6, 167.2, 166.2, 161.9, 159.6 (d, *J*_{CCF} = 26.1 Hz), 156.3, 151.0, 141.4 (d, *J*_{CF} = 232.5 Hz), 133.7, 130.5 (d, *J*_{CCF} = 33.1 Hz), 130.4 (2C), 116.0 (2C), 107.6, 102.1, 97.1, 95.2, 78.4, 74.7, 72.1, 71.7, 71.6, 71.2, 71.1, 70.4, 69.0, 62.5, 49.8, 47.0, 40.8, 39.4, 37.3, 34.3, 32.0, 30.6, 28.0, 26.9, 25.0 ppm; HRMS (ESI TOF-MS) C₄₂H₅₂FN₃O₁₈SNa⁺ [M + Na]⁺ calc. 960.2843, found 960.2847.

(5-Fluoro-2,4-dioxo-3,4-dihydropyrimidin-1(2H)-yl)methyl 6-((2-(2-(2-(3,5-dihydroxy-4-(3-(4-hydroxyphenyl)propanoyl)phenoxy)ethoxy)ethoxy)ethyl)thio)-2,5-dioxopyrrolidin-1-yl)hexanoate (5). To a solution of 17 (22 mg, 0.05 mmol) in dry MeOH (1 mL) was added 22 (19 mg, 0.05 mmol). The reaction mixture was stirred for 10 min and then was concentrated *in vacuo*. The residue was purified by column chromatography (silica gel; DCM/MeOH = 12/1) to give 5 (39 mg, 0.05 mmol, >99%) as foam. ¹H NMR (400 MHz, CD₃OD) δ 7.89 (d, *J* = 6 Hz, 1H, H-29), 7.05 (d, *J* = 8.4 Hz, 2H, H-2, H-6), 6.68 (d, *J* = 8.4 Hz, 2H, H-3, H-5), 5.92 (s, 2H, H-3', H-5'), 5.61 (s, 2H), 4.09 (t, *J* = 4.4 Hz, 2H), 4.09–3.99 (m, 1H), 3.81 (t, *J* = 4.4 Hz, 2H), 3.76–3.72 (m, 2H), 3.69–3.64 (m, 4H), 3.42 (t, *J* = 7 Hz, 2H), 3.21–3.20 (m, 1H), 3.11–3.07 (m, 2H), 2.87–2.83 (m, 3H), 2.47 (dd, *J* = 14.8, 3.6 Hz, 1H), 2.34 (t, *J* = 7.3 Hz, 2H), 1.62–1.50 (m, 4H), 1.29–1.27 (m, 2H) ppm; ¹³C NMR (100 MHz, CD₃OD) δ 206.7, 178.9, 177.1, 174.5, 166.5, 165.5 (2C), 159.7 (d, *J*_{CCF} = 27.4 Hz), 156.4, 151.3, 141.6 (d, *J*_{CF} = 227 Hz), 133.8, 130.5 (d, *J*_{CCF} = 32.2 Hz), 130.3 (2C), 116.1 (2C), 106.1, 94.8 (2C), 72.1, 71.7, 71.6, 71.2, 70.4, 68.7, 47.4, 40.7, 39.4, 37.2, 34.3, 32.0, 31.2, 28.0, 26.9, 25.0 ppm; HRMS (ESI TOF-MS) C₃₆H₄₂FN₃O₁₃SNa⁺ [M + Na]⁺ calc. 798.2315, found 798.2319.

(5-Fluoro-2,4-dioxo-3,4-dihydropyrimidin-1(2H)-yl)methyl 4-((2-(2-(2-(3-hydroxy-4-(3-(4-hydroxyphenyl)propanoyl)-5-(((2S,3R,5S,6R)-3,4,5-trihydroxy-6-(hydroxymethyl)-tetrahydro-2H-pyran-2-yl)oxy)phenoxy)ethoxy)ethoxy)ethyl)-disulfanyl)butanoate (6). To a solution of compound 16 (76 mg, 0.13 mmol) in THF were added compound 23 (50 mg, 0.13 mmol) and

phosphate buffer (pH = 8.0). The mixture was stirred for 2 h at ambient temperature. The solvent was removed *in vacuo*. The residue was purified by column chromatography (silica gel; DCM/MeOH = 15/1 to 10/1) to give compound 6 (107 mg, 0.13 mmol, >99%) as oil; ¹H NMR (400 MHz, CD₃OD) δ 7.89 (t, *J* = 6.1 Hz, 1H), 7.07 (t, *J* = 8.4 Hz, 2H), 6.68 (t, *J* = 8.4 Hz, 2H), 6.32 (d, *J* = 2.2 Hz, 1H), 6.13 (d, *J* = 2.2 Hz, 1H), 5.62 (s, 2H), 5.10–5.03 (m, 1H), 4.64 (t, *J* = 7.2 Hz, 1H), 4.17–4.05 (m, 2H), 3.90 (dd, *J* = 12.4 Hz, 2.0 Hz, 1H), 3.83–3.95 (m, 2H), 3.59–3.73 (m, 7H), 3.44–3.54 (m, 6H), 3.34–3.39 (m, 1H), 2.87 (m, 4H), 2.72 (t, *J* = 7.0 Hz, 2H), 2.49 (t, *J* = 7.0 Hz, 2H), 1.98 (t, *J* = 7.0 Hz, 2H); ¹³C NMR (100 MHz, CD₃OD) δ 205.5, 172.9, 166.0, 165.0, 160.6, 159.8 (d, *J*_{CCF} = 27 Hz), 155.0, 149.8, 140.0 (d, *J*_{CF} = 233 Hz), 132.4, 129.3 (d, *J*_{CCF} = 35 Hz), 129.1 (2C), 114.7 (2C), 106.3, 100.8, 95.8, 93.8, 77.1, 77.1, 73.4, 70.0 (2C), 69.8, 69.5 (2C), 67.6, 66.3, 61.1, 45.8, 38.0, 37.3, 31.7, 29.3, 23.6 ppm; HRMS (ESI TOF-MS) C₃₆H₄₅FN₂O₁₆S₂⁺ [M + H]⁺ calc. 845.2267, found 845.2279.

(5-Fluoro-2,4-dioxo-3,4-dihydropyrimidin-1(2H)-yl)methyl 4-((2-(2-(2-(3,5-dihydroxy-4-(3-(4-hydroxyphenyl)propanoyl)phenoxy)ethoxy)ethoxy)ethyl)disulfanyl)butanoate (7). To a solution of compound 17 (55 mg, 0.13 mmol) in THF were added compound 23 (50 mg, 0.13 mmol) and phosphate buffer (pH 8.0). The mixture was stirred for 2 h at ambient temperature. The solvent was removed *in vacuo*. The residue was purified by column chromatography (silica gel; DCM/MeOH = 20/1) to give compound 7 (85 mg, 0.12 mmol, 92%) as a solid; ¹H NMR (600 MHz, *d*₆-acetone) δ 7.93 (d, *J* = 6.4 Hz, 1H), 7.09 (d, *J* = 8.4 Hz, 2H), 6.75 (d, *J* = 9.4 Hz, 2H), 5.69 (s, 2H), 6.01 (s, 2H), 4.15 (t, *J* = 4.6 Hz, 2H), 3.81 (t, *J* = 4.3 Hz, 2H), 3.70 (t, *J* = 6.5 Hz, 2H), 3.66–3.60 (m, 4H), 3.35 (t, *J* = 8.0 Hz, 2H), 2.89–2.77 (m, 4H), 2.78 (t, *J* = 7.2 Hz, 2H), 2.52 (t, *J* = 7.2 Hz, 2H), 2.07–2.04 (m, 2H); ¹³C NMR (150 MHz, *d*₆-acetone) δ 205.8, 173.3, 166.1, 165.3, 157.9 (d, *J*_{CCF} = 27 Hz), 156.4, 150.1, 140.9 (d, *J*_{CF} = 231 Hz), 133.4, 130.2 (2C), 129.0 (d, *J*_{CCF} = 34.5 Hz), 115.2 (2C), 105.7, 94.0 (2C), 71.4, 71.3, 71.0, 70.1, 70.0, 68.5, 47.0, 39.3, 38.1, 32.7, 30.5, 30.3, 24.7 ppm. HRMS (ESI TOF-MS) C₃₀H₃₅FN₂O₁₁S₂⁺ [M + H]⁺ calc. 683.1739, found 683.1763.

(5-Fluoro-2,4-dioxo-3,4-dihydropyrimidin-1(2H)-yl)methyl 3-(1-(2-(2-(2-(3-hydroxy-4-(3-(4-hydroxyphenyl)propanoyl)-5-(((2S,3R,5S,6R)-3,4,5-trihydroxy-6-(hydroxymethyl)-tetrahydro-2H-pyran-2-yl)oxy)phenoxy)ethoxy)ethoxy)ethyl)-1H-1,2,3-triazol-4-yl)propanoate (8). To a solution of 20 (95 mg, 0.16 mmol) in EtOH/water (3/1, 2 mL) were added TBTA (18 mg, 0.03 mmol), sodium ascorbic acid (20.8 mg, 0.10 mmol), copper(II) sulfate pentahydrate (3.3 mg, 0.01 mmol), and 24 (38 mg, 0.16 mmol). The reaction mixture was stirred for 12 h and then concentrated *in vacuo*. The mixture was dissolved in EtOAc and was extracted with water. The organic layers were concentrated *in vacuo* and purified by column chromatography (silica gel; DCM/MeOH = 10/1) to give 8 (117 mg, 0.14 mmol, 88%) as foam. ¹H NMR (600 MHz, CD₃OD) δ 7.81 (d, *J* = 6 Hz, 1H, H-24), 7.77 (s, 1H, H-13), 7.06 (d, *J* = 8.4 Hz, 2H, H-2, H-6), 6.67 (d, *J* = 8.4 Hz, 2H, H-3, H-5), 6.30 (d, *J* = 2.4 Hz, 1H, H-3'), 6.12 (d, *J* = 2.4 Hz, 1H, H-5'), 5.59 (s, 2H, H-18), 5.07 (d, *J* = 7.2 Hz, 1H, H-1''), 4.50 (t, *J* = 4.8 Hz, 2H, H-12), 4.15 (t, *J* = 4.2 Hz, 2H, H-7), 3.88 (dd, *J* = 10, 2 Hz, 1H), 3.80 (t, *J* = 4.8 Hz, 2H), 3.79–3.77 (m, 2H), 3.68 (q, *J* = 6 Hz, 1H), 3.66–3.61 (m, 4H), 3.5–3.4 (m, 5H), 3.38–3.34 (m, 1H), 2.94 (t, *J* = 7.8 Hz, 2H, H-16), 2.88 (t, *J* = 7.2 Hz, 2H, H- β), 2.72 (t, *J* = 7.2 Hz, 2H, H-17) ppm; ¹³C NMR (150 MHz, CD₃OD) δ 206.8, 173.5, 167.2, 166.2, 161.8, 159.5 (d, *J*_{CCF} = 26 Hz), 156.4, 150.9, 146.9, 141.3 (d, *J*_{CF} = 232 Hz), 133.7, 130.5 (d, *J*_{CCF} = 34 Hz), 130.3 (2C), 124.4, 116.0 (2C), 107.6, 102.1, 97.1, 95.1, 78.5, 78.4, 74.7, 71.6, 71.5, 71.4, 71.1, 70.4, 70.3, 68.9, 62.4, 51.3, 47.0, 34.0, 30.6, 21.4 ppm; HRMS (ESI TOF-MS) C₃₇H₄₅FN₃O₁₆⁺ [M + H]⁺ calc. 834.2840, found 834.2855.

(5-Fluoro-2,4-dioxo-3,4-dihydropyrimidin-1(2H)-yl)methyl 3-(1-(2-(2-(2-(3-hydroxy-4-(3-(4-hydroxyphenyl)propanoyl)-5-(((2S,3R,5S,6R)-3,4,5-trihydroxy-6-(hydroxymethyl)-tetrahydro-2H-pyran-2-yl)oxy)phenoxy)ethoxy)ethoxy)ethyl)-1H-1,2,3-triazol-4-yl)propanoate (9). To a solution of 21 (62.3 mg, 0.14 mmol) in EtOH/water (3: 1, 2 mL) were added TBTA (7.9 mg, 0.01 mmol), sodium ascorbic acid (45 mg, 0.22 mmol), copper(II) sulfate pentahydrate (5.6 mg, 0.02 mmol), and 24 (35.7 mg, 0.15 mmol). The reaction mixture was stirred for 12 h and then concentrated

in vacuo. The mixture was then dissolved in EtOAc and was extracted with water. The organic layers were concentrated in vacuo and purified by column chromatography (silica gel; DCM/MeOH = 14/1) to give **9** (62.9 mg, 0.09 mmol, 64%) as foam; ^1H NMR (400 MHz, d_6 -DMSO) δ 8.11 (d, J = 6.4 Hz, 1H, H-24), 7.85 (s, 1H, H-13), 7.05 (d, J = 8.4 Hz, 2H, H-2, H-6), 6.69 (d, J = 8.4 Hz, 2H, H-3, H-5), 5.96–5.96 (m, 2H, H-3', H-5'), 5.59 (s, 2H, H-18), 4.48 (t, J = 5 Hz, 2H, H-12), 4.12–4.05 (m, 2H), 3.82 (t, J = 5 Hz, 2H), 3.75–3.65 (m, 2H), 3.59–3.51 (m, 4H), 3.27 (t, J = 7.6 Hz, 2H), 2.89 (t, J = 7.2 Hz, 2H, H-16), 2.80 (t, J = 7.4 Hz, 2H, H- β), 2.7 (t, J = 7.2 Hz, 2H, H-17) ppm; ^{13}C NMR (100 MHz, CD_3OD) δ 206.7, 173.6, 166.5, 165.6 (2C), 159.7 (d, J_{CCF} = 26 Hz), 156.5, 151.1, 147.0, 141.3 (d, J_{CF} = 232 Hz), 133.9, 130.4 (d, J_{CCF} = 34 Hz), 130.3 (2C), 124.4, 116.1 (2C), 106.1, 94.8 (2C), 71.6, 71.6, 71.4, 70.5, 70.3, 68.7, 51.3, 47.4, 34.0, 31.2, 21.5 ppm; HRMS (ESI TOF-MS) $\text{C}_{31}\text{H}_{35}\text{FN}_5\text{O}_{11}^+ [\text{M} + \text{H}]^+$ calc. 672.2312, found 672.2318.

1-(4-(2-(2-(2-(tert-Butyldisulfanyl)ethoxy)ethoxy)ethoxy)-2-hydroxy-6-(((2S,3R,5S,6R)-3,4,5-trihydroxy-6-(hydroxymethyl)tetrahydro-2H-pyran-2-yl)oxy)phenyl)-3-(4-hydroxyphenyl)propan-1-one (15). Phlorizin (1.0 g, 2.29 mmol) in dry DMF (10 mL) was added K_2CO_3 (436 mg, 3.15 mmol) at ambient temperature and stirred for 10 min. Compound **14** (1.0 g, 3.16 mmol, see the Supporting Information) was added, and the reaction mixture was heated at 55 °C for 12 h. The reaction mixture was concentrated in vacuo. The residue was extracted with water/EtOAc three times. The organic layers were combined and concentrated in vacuo. The residue was purified by column chromatography (silica gel; DCM/MeOH = 10/1) to give compound **15** (837 mg, 1.25 mmol, 54%) as foam; ^1H NMR (400 MHz, CD_3OD) δ 7.06 (d, J = 8.4 Hz, 2H, H-2, H-6), 6.68 (d, J = 8.4 Hz, 2H, H-3, H-5), 6.33 (d, J = 2.4 Hz, 1H, H-3'), 6.14 (d, J = 2.4 Hz, 1H, H-5'), 5.08 (d, J = 7.6 Hz, 1H, H-1''), 4.15 (t, J = 4.4 Hz, 2H), 3.91–3.88 (m, 1H), 3.82 (t, J = 4.4 Hz, 2H), 3.71–3.62 (m, 5H), 3.61–3.60 (m, 2H), 3.50–3.44 (m, 5H), 3.34 (d, J = 9.2 Hz, 1H), 2.90–2.84 (m, 4H), 1.30 (s, 9H, H-14, H-15, H-16) ppm; ^{13}C NMR (150 MHz, CD_3OD) δ 206.8, 167.2, 166.2, 161.8, 156.3, 133.7, 130.3 (2C), 116.0 (2C), 107.6, 102.1, 97.1, 95.1, 78.4, 74.7, 71.6, 71.3, 71.1, 70.7, 70.5, 68.9, 62.4, 48.4, 47.0, 40.9, 30.6, 30.2 (3C) ppm; HRMS (ESI TOF-MS) $\text{C}_{31}\text{H}_{44}\text{NaO}_{12}\text{S}_2\text{Na}^+ [\text{M} + \text{Na}]^+$ calc. 695.2166, found 695.2174.

1-(2-Hydroxy-4-(2-(2-(2-mercaptoethoxy)ethoxy)ethoxy)-6-(((2S,3R,5S,6R)-3,4,5-trihydroxy-6-(hydroxymethyl)tetrahydro-2H-pyran-2-yl)oxy)phenyl)-3-(4-hydroxyphenyl)propan-1-one (16). To a stirred solution of **15** (156 mg, 0.23 mmol) in dry THF (5 mL) were added TCEP (133 mg, 0.46 mmol) and 4.0 N NaOH solution (1 mL). The reaction mixture was stirred for 5 h and then was concentrated in vacuo. The residue was dissolved in EtOAc, and the precipitate was filtered. The filtrate was concentrated in vacuo and was purified by column (silica gel; DCM/MeOH = 10/1) to give compound **16** (115 mg, 0.20 mmol, 86%) as foam; ^1H NMR (400 MHz, CD_3OD) δ 7.06 (d, J = 8.4 Hz, 2H, H-2, H-6), 6.68 (d, J = 8.4 Hz, 2H, H-3, H-5), 6.33 (d, J = 2.4 Hz, 1H, H-3'), 6.14 (d, J = 2.4 Hz, 1H, H-5'), 5.08 (d, J = 7.2 Hz, 1H, H-1''), 4.15 (t, J = 4.4 Hz, 1H, H-7), 3.91 (dd, J = 10, 2 Hz, 1H), 3.84–3.81 (m, 2H), 3.71–3.68 (m, 3H), 3.64–3.62 (m, 2H), 3.59 (t, J = 6.4 Hz, 2H), 3.50–3.43 (m, 5H), 3.39–3.37 (m, 1H), 2.88 (t, J = 7.5 Hz, 2H), 2.64 (t, J = 6.4 Hz, 2H) ppm; ^{13}C NMR (100 MHz, CD_3OD) δ 206.8, 167.3, 166.3, 161.8, 156.3, 133.7, 130.3 (2C), 116.0 (2C), 107.6, 102.1, 97.1, 95.1, 78.5, 78.4, 74.7, 74.1, 71.6, 71.1 (2C), 70.5, 68.9, 62.4, 47.0, 30.7, 24.6 ppm; HRMS (ESI TOF-MS) $\text{C}_{27}\text{H}_{36}\text{O}_{12}\text{SNa}^+ [\text{M} + \text{Na}]^+$ calc. 607.1820, found 607.1821.

1-(2,6-Dihydroxy-4-(2-(2-(2-mercaptoethoxy)ethoxy)ethoxy)phenyl)-3-(4-hydroxyphenyl)propan-1-one (17). To a solution of compound **16** (210 mg, 0.36 mmol) in EtOH (2 mL) was added 1.0 N HCl (1 mL). The mixture was heated at reflux for 3 h. The reaction mixture was cooled, and the solvent was evaporated in vacuo. The residue was extracted with water and EtOAc and dried over MgSO_4 . The organic layers were combined and concentrated in vacuo. The residue was purified by column chromatography (silica gel; Hex/EtOAc = 1/1) to give compound **17** (111 mg, 0.26 mmol, 73%) as foam; ^1H NMR (400 MHz, CDCl_3) δ 7.00 (d, J = 8.4 Hz, 2H, H-2, H-6), 6.70 (d, J = 8.4 Hz, 2H, H-3, H-5), 5.87 (s, 2H, H-3', H-5'), 4.00 (t, J = 3.2 Hz, 2H), 3.79–3.77 (m, 2H), 3.71–3.69 (m, 2H), 3.63–3.61 (m,

2H), 3.54 (t, J = 6.4 Hz, 2H), 3.27 (t, J = 7.6 Hz, 2H), 2.83 (t, J = 7.6 Hz, 2H), 2.62–2.57 (m, 2H); ^{13}C NMR (100 MHz, CDCl_3) δ 205.2, 164.5 (2C), 153.7, 133.4, 129.5 (2C), 115.3 (2C), 94.5 (2C), 77.2, 72.8, 70.4, 70.4, 69.9, 69.4, 67.0, 45.8, 29.8, 23.9; HRMS (ESI TOF-MS) $\text{C}_{21}\text{H}_{26}\text{O}_7\text{SNa}^+ [\text{M} + \text{Na}]^+$ calc. 445.1291, found 445.1328.

1-(4-(2-(2-(2-Azidoethoxy)ethoxy)ethoxy)-2-hydroxy-6-(((2S,3R,5S,6R)-3,4,5-trihydroxy-6-(hydroxymethyl)tetrahydro-2H-pyran-2-yl)oxy)phenyl)-3-(4-hydroxyphenyl)propan-1-one (20). Phlorizin (2.31 g, 5.30 mmol) in dry DMF (15 mL) was added K_2CO_3 (1.11 g, 8.03 mmol) at ambient temperature and stirred for 10 min. Compound **19** (1.66 g, 7.00 mmol, see the Supporting Information for its preparation) was added, and the reaction mixture was heated at 55 °C for 12 h. The reaction mixture was concentrated in vacuo. The residue was extracted with water/EtOAc three times. The organic layers were combined and concentrated in vacuo. The residue was purified by column chromatography (silica gel; DCM/MeOH = 10/1) to give compound **20** (2.13 g, 3.59 mmol, 68%) as foam; ^1H NMR (600 MHz, CD_3OD) δ 7.08 (d, J = 8.4 Hz, 2H, H-2, H-6), 6.70 (d, J = 8.4 Hz, 2H, H-3, H-5), 6.34 (d, J = 2.4 Hz, 1H, H-3'), 6.15 (d, J = 2.4 Hz, 1H, H-5'), 5.10 (d, J = 7.2 Hz, 1H, C-1''), 4.16 (t, J = 4.4 Hz, 2H, H-9), 3.91 (d, J = 2 Hz, 1H), 3.83 (t, J = 4.4 Hz, 1H), 3.73–3.70 (m, 5H), 3.69–3.67 (m, 1H), 3.52–3.50 (m, 4H), 3.49–3.40 (m, 5H), 2.90 (t, J = 7.8 Hz, 2H, H-12) ppm; ^{13}C NMR (150 MHz, CD_3OD) δ 206.8, 167.2, 166.2, 161.8, 156.3, 133.7, 130.3 (2C), 116.0 (2C), 107.6, 102.1, 97.1, 95.1, 78.4, 74.7, 71.7, 71.3, 71.1, 70.7, 70.5, 68.9, 62.4, 51.7, 47.0, 30.6 ppm; HRMS (ESI TOF-MS) $\text{C}_{27}\text{H}_{35}\text{N}_3\text{O}_{12}\text{Na}^+ [\text{M} + \text{Na}]^+$ calc. 616.2113, found 616.2115.

1-(4-(2-(2-(2-Azidoethoxy)ethoxy)ethoxy)-2,6-dihydroxyphenyl)-3-(4-hydroxyphenyl)propan-1-one (21). To a solution of compound **20** (195 mg, 0.33 mmol) in EtOH (5 mL) was added 1.0 N HCl (3 mL). The mixture was refluxed at 90 °C for 3 h. The reaction mixture was cooled, and the solvent was evaporated in vacuo. The residue was extracted with water/EtOAc and dried with MgSO_4 . The organic layers were combined and concentrated in vacuo. The residue was purified by column chromatography (silica gel; Hex/EtOAc = 1/1) to give compound **21** (110 mg, 0.26 mmol, 79%) as foam; ^1H NMR (400 MHz, CDCl_3) δ 7.04 (d, J = 8.4 Hz, 2H, C-2, C-6), 6.71 (d, J = 8.4 Hz, 2H, C-3, C-5), 5.95–5.85 (m, 2H, C-3', C-5'), 4.06–4.04 (m, 2H, C-7), 3.82 (t, J = 4.4 Hz, 2H), 3.73–3.70 (m, 2H), 3.67–3.65 (m, 2H), 3.60 (t, J = 5 Hz, 2H), 3.33–3.28 (m, 4H, C- α , C-12), 2.89 (t, J = 7.7 Hz, 2 Hz, C- β) ppm; ^{13}C NMR (100 MHz, CDCl_3) δ 204.9, 164.5 (2C), 153.7, 133.7, 129.5 (2C), 115.2 (2C), 105.0, 94.6 (2C), 70.6, 70.4, 69.9, 69.8, 67.1, 50.5, 45.8, 29.7 ppm; HRMS (ESI TOF-MS) $\text{C}_{21}\text{H}_{25}\text{N}_3\text{O}_7\text{Na}^+ [\text{M} + \text{Na}]^+$ calc. 454.1585, found 454.1583.

1-(6-Maleimidohexanoyloxymethyl)-5-fluorouracil (22). To a solution of 5-FU (100 mg, 0.77 mmol) in water (0.5 mL) was added formaldehyde (37%, 0.5 mL) at 60 °C and stirred for another 3 h after the solids completely disappeared. Then, the solvent was removed in vacuo to obtain colorless and viscous oil. In another flask, to 6-maleimidohexanoic acid (195 mg, 0.92 mmol) in dry ACN (2 mL) were added DCC (190 mg, 0.92 mmol) and DMAP (9.5 mg, 0.08 mmol) at 0 °C and stirred for 10 min. Then, the abovementioned oil in dry ACN (0.5 mL) was added to the reaction flask. The reaction mixture was stirred at 0 °C for 30 min and then stirred at room temperature for 12 h. The precipitates formed in the reaction were filtered, and the filtrate was evaporated in vacuo. The residue in EtOAc was extracted with 1.0 N HCl, saturated NaHCO_3 , and water. The organic layers were dried over MgSO_4 and concentrated in vacuo. The residue was purified by column chromatography (silica gel; Hex/EtOAc = 1/1) to give compound **22** (117 mg, 0.33 mmol, 43%) as foam. ^1H NMR (600 MHz, CD_3OD) δ 7.92 (d, J = 6 Hz, 1H, H-6), 6.79 (s, 2H, H-16, H-17), 5.63 (s, 2H, H-7), 3.48 (t, J = 6.9 Hz, 2H, H-13), 2.38 (t, J = 7.3 Hz, 2H, H-9), 1.68–1.63 (m, 2H, H-10), 1.59–1.54 (m, 2H, H-12), 1.32–1.27 (m, 2H, H-11); ^{13}C NMR (150 MHz, CD_3OD) δ 174.6, 172.5 (2C), 159.7 (d, J_{CCF} = 25 Hz), 151.1, 141.4 (d, J_{CF} = 233 Hz), 135.3 (2C), 130.5 (d, J_{CCF} = 34 Hz), 71.6, 38.2, 34.3, 29.1, 27.0, 25.1; HRMS (ESI TOF-MS) $\text{C}_{15}\text{H}_{16}\text{FN}_3\text{O}_6\text{C}_{21}\text{Na}^+ [\text{M} + \text{Na}]^+$ calc. 376.0915, found 376.0915.

1-(4-(Pyridin-2-yl)disulfanyl)butyroyloxymethyl)-5-fluorouracil (23). A solution of 5-FU (100 mg, 0.77 mmol) in 37% formaldehyde solution (0.5 mL) was stirred at 60 °C until the solids

completely disappeared and was stirred at 60 °C for another 3 h. The solvent was removed in vacuo to obtain a colorless oil. In another flask were added 4-(2-pyridyldithio)butanoic acid (206 mg, 0.90 mmol), DCC (190 mg, 0.92 mmol), and DMAP (11 mg, 0.09 mmol) in ACN (5 mL) at 0 °C, and the reaction was stirred for 10 min. Then, the solution was added to the abovementioned colorless oil. The reaction mixture was stirred at 0 °C for 30 min and then stirred at room temperature for 12 h. The precipitates formed in the reaction were filtered, and the filtrate was evaporated in vacuo. The residue in EtOAc was extracted with 1.0 N HCl, saturated NaHCO₃, and water. The organic layers were dried over MgSO₄ and concentrated in vacuo. The residue was purified by column chromatography (silica gel; CHCl₃/MeOH = 25/1) to give compound 23 (95.5 mg, 0.26 mmol, 34%, two steps) as a solid; ¹H NMR (400 MHz, CDCl₃) δ 8.41 (d, *J* = 4.8 Hz, 1H), 7.62 (t, *J* = 7.3 Hz, 2H), 7.58 (d, *J* = 5.4 Hz, 1H), 7.11–7.01 (m, 1H), 5.60 (s, 2H), 2.78 (t, *J* = 7 Hz, 2H), 2.50 (t, *J* = 7.2 Hz, 2H), 1.21–1.91 (m, 2H); ¹³C NMR (100 MHz, CDCl₃) δ 173.1, 159.8 (d, *J*_{CCF} = 27 Hz), 156.9, 149.8, 149.3, 140.3 (d, *J*_{CF} = 238 Hz), 137.2, 128.5 (d, *J*_{CCF} = 24 Hz), 120.9, 120.0, 69.8, 37.6, 32.2, 23.5 ppm; HRMS (ESI TOF-MS) C₁₄H₁₅F₃N₃O₄S₂⁺ [M + H]⁺ calc. 372.0485, found 372.0483.

1-(Pent-4-ynoyloxymethyl)-5-fluorouracil (24). A solution of 5-FU (100 mg, 0.77 mmol) in 37% formaldehyde solution (0.5 mL) was stirred at 60 °C until the solids completely disappeared and was stirred at 60 °C for another 3 h. The solvent was removed in vacuo to obtain a colorless oil. In another flask was added pent-4-ynoic acid (105 mg, 1.07 mmol), DCC (285 mg, 1.38 mmol), and DMAP (11 mg, 0.09 mmol) in ACN (5 mL) at 0 °C and the reaction was stirred for 10 min to give pre-activated pent-4-ynoic acid. Then, pre-activated pent-4-ynoic acid in ACN was added to the abovementioned colorless oil. The reaction mixture was stirred at 0 °C for 30 min and then stirred at room temperature for 12 h. The solids were filtered, and the filtrate was evaporated in vacuo. The residue in EtOAc was extracted with 1.0 N HCl, saturated NaHCO₃ solution, and water sequentially. The organic layers were dried over MgSO₄, concentrated in vacuo, and purified by column chromatography (silica gel; Hex/EtOAc = 2/1) to give compound 24 (118 mg, 0.49 mmol, 63%) as amorphous solids; ¹H NMR (400 MHz, CDCl₃) δ 7.59 (d, *J* = 5.4 Hz, 1H, H-6), 5.65 (s, 2H, H-7), 2.67–2.55 (m, 2H), 2.54–2.46 (m, 2H), 1.97 (t, *J* = 2.5 Hz, 1H, H-12) ppm; ¹³C NMR (150 MHz, CDCl₃) δ 171.9, 156.4 (d, *J*_{CCF} = 28 Hz), 148.8, 140.1 (d, *J*_{CF} = 237 Hz), 128.3 (d, *J*_{CCF} = 33 Hz), 81.5, 69.7, 69.5, 32.9, 14.1 ppm; HRMS (ESI TOF-MS) C₁₀H₉FN₂O₄Na⁺ [M + Na]⁺ calc. 263.0439, found 263.0443.

Cell Culture and Cytotoxic Assay. Cancer cell lines were obtained from ATCC unless otherwise noted. HT-29 and HCT-116 cells were cultured in Dulbecco's Modified Eagle Medium (DMEM, Thermo Fisher Scientific) with 10% fetal bovine serum (FBS, Thermo Fisher Scientific) and 1% antibiotic–antimycotic (Thermo Fisher Scientific). Normal cell line NHDF cells were obtained from PromoCell unless otherwise noted. NHDF cells were cultured in Dulbecco's Modified Eagle Medium (DMEM, Sigma-Aldrich, Product # 6429) with 10% fetal bovine serum (FBS, Thermo Fisher Scientific) and 1% antibiotic–antimycotic (Thermo Fisher Scientific). The cells were incubated at 37 °C in a humidified incubator with 5% CO₂ and 95% air.

Cytotoxicity of the compounds against HT-29, HCT-116, and NHDF cells was determined by SRB assay. Briefly, CRC cells were seeded at a density of 5 × 10³ cells/well in 96-well microtiter plates (100 μL/well), separated into two groups with or without GSH. After incubation for 24 h, the culture medium was replaced by fresh medium (100 μL). For non-GSH control groups, a series of concentrations of compounds (100 μL, diluted by medium) were added to cells directly; for GSH groups, cells were transiently treated with 30 mM GSH (20 μL/well, diluted by medium) for 1 h, and then a series of concentration of compounds (40 μL/well) and 10 mM GSH (40 μL/well) were added, making the final GSH concentration 5 mM, and incubated for 48 h. After incubation, 10% cold trichloroacetic acid was gently added to each well and incubated at 4 °C for 1 h. The medium was removed, carefully washed with water, and dried at room temperature. Next, plates were stained with 100 μL of 0.057% SRB for 30 min, rinsed with 1% acetic acid to remove the unbound dye, and dried at room

temperature. The bound protein stain was dissolved with 100 μL of 10 mM Tris base (pH 10.5) and shaken for 10 min. Optical density (O.D.) was measured at 510 nm with a multimode microplate reader (SpectraMax Paradigm, Beckman Coulter, U.S.). The fraction of cell survival was calculated as follows: survival fraction = (OD treated – blank)/(OD control – blank). IC₅₀ values (the concentrations that produce 50% inhibition of cell growth) were calculated using nonlinear regression curve-fitting models (GraphPad Prism 7, U.S.). Each experiment was repeated three times.

2-NBDG Uptake Assay. COS-7 cells were seeded in 96-well culture plates and grown in low-glucose Dulbecco's Modified Eagle's Medium supplemented with 10% fetal bovine serum and 2 mM L-glutamine for 24 h. After washing with Krebs Ringer bicarbonate buffer (KRB) (10 mM HEPES, 129 mM NaCl, 4.7 mM KCl, 2 mM CaCl₂, 1.2 mM MgSO₄, 1.2 mM KH₂PO₄, and 5 mM NaHCO₃, pH 7.4), cells were incubated with the compounds to be tested in KRB containing 2-NBDG (200 μM) for 90 min at 37 °C in a 5% CO₂ atmosphere, then washed twice with KRB, and lysed with lysis buffer (1% Nonidet P-40, 1% sodium deoxycholate, 40 mM KCl, and 20 mM Tris, pH 7.4). Finally, the lysates were transferred to black 96-well plates and fluorescence intensity was detected with a multimode microplate reader (SpectraMax Paradigm, Beckman Coulter, USA) using an excitation wavelength of 475 nm and an emission wavelength of 550 nm.²²

In Vivo Studies. Specific pathogen-free BALB/c mice (6 weeks of age, male) were purchased from the National Laboratory Animal Center. The animals were housed in clean plastic microisolator cages (five mice/cage), maintained on standard laboratory pellet diet and water ad libitum. Animal rooms were kept at constant temperature, humidity, and 12 h dark/light cycle. All animal procedures were in accordance with the recommendations of the Committee for the Laboratory Animal Care Committee in National Taiwan University College of Medicine [IACUC 20180076].

The azoxymethane (AOM)-induced murine CRC model was applied to model human CRC. BALB/c mice (6 weeks of age, male) were intraperitoneally (i.p.) injected once every 2 weeks with AOM (10 mg/kg body weight) or the PBS vehicle. Seven days after each AOM injection, 2% dextran sulfate sodium (DSS) was given in the drinking water for 4 days followed by 3 days of regular water. This cycle was repeated three times. The mice were randomly divided into four groups (*n* = 5) on day 60 after the first AOM treatment. 5-FU (50 mg/kg body weight), compound 7 (50 mg/kg body weight each), and 5-FU + 17 (5-FU (10 mg/kg) and 17 (30 mg/kg)) in 0.2 mL of PBS were injected i.p. once every 3 days for 3 weeks. Body weight was measured every 3 days. The mice were sacrificed on day 21 after the first treatment. Tumor volumes and body weights were recorded at sacrifice. The numbers of tumors were determined under a dissecting microscope, and the area covered by tumors was measured by imaging software (AxioVision LE 4.8.2.0).

In the following PK experiments, BALB/c mice (6 weeks of age, male) were randomly divided into two groups (*n* = 3). The two groups of mice were treated with 5-FU solution (9.5 mg/kg) and compound 7 (50 mg/kg, equivalent as 5-FU), respectively, by intraperitoneal and intravenous injection. Blood samples were collected via femoral vein by syringes at 0, 1, 3, 5, 10, 15, 30, and 45 min and 1, 2, 4, and 24 h after drug administration. A total of 50 μL of blood samples was collected into 100 μL of extraction solvent (EtOAc/MeOH, 1:1) and vortexed for 30 s. The supernatants were separated from the mixture by centrifugation at 10,000 rpm for 10 min and frozen at –30 °C, pending UPLC-MS/MS analysis. For biodistribution experiments, the entire dissected organs were placed into weight-known 2 mL microcentrifuge tubes with 1 mL of extraction solvent (EtOAc/MeOH, 1:1) and 7 mm stainless steel beads and then homogenized for 30 min. All of the containers were maintained at 4 °C throughout the processes. The supernatants were separated from the mixture by centrifugation at 10,000 rpm for 10 min and frozen at –30 °C. The 200 μL solvent from crude organ suspensions was removed using a dryer, and then they were dissolved in 50 μL of extraction solvent. All samples were stored at –30 °C and analyzed within 24 h. All of the samples were filtered through 0.22 μm PTFE membranes into 12 × 32 mm vials for UPLC-MS/MS analyses using 5-FU-¹⁵N₂ as a marker. Pharmacokinetic parameters

were calculated using the WinNonlin Software (version 5.2, Pharsight, MO, USA.)

UPLC-MS/MS Analyses. Analyses were performed on a ACQUITY UPLC I-Class/Xevo TQ-XS IVD System (Waters, Milford, MA, USA) from College of Public Health, National Taiwan University. The reverse phase BEH C18 (100 mm × 2.1 mm, 1.7 μm, Waters) and VanGuard BEH C18 (5 mm × 2.1 mm, 1.7 μm, Waters) precolumns were used to separate the analytes. All data were acquired by MassLynx V4.2. The mobile phase consisted of a 10 mM aqueous solution of ammonium acetate (A) and acetonitrile (B), set as follows: 0.00 min 98% A → 1.00 min 98% A → 3.00 min 10% A → 4.50 min 10% A → 4.60 min 98% A → 6.00 min 98% A, at a rate of 0.5 mL/min for 6.00 min with 4 μL per injection. The column oven was maintained at 60 °C. A multiple reaction monitoring (MRM) method was applied in quantification. Mass spectrometer parameters were as follows: capillary voltage, 3.0 kV/3.0 kV, respectively, for positive/negative ion mode; ion source temperature, 120 °C; desolvation temperature, 450 °C; cone gas flow (N₂), 50 L/h; desolvation gas flow (N₂), 700 L/h; multiplier, 650 V; and collision gas pressure (Ar), 3–4 × 10⁻³ mbar. Other parameters are listed in Table S1.

Plasma Stability and Drug Releasing Assay. To access human plasma stability, synthesized conjugates were dissolved in DMSO, and the analysis solutions were prepared by diluting 1 μL of stock with 4 μL of PBS (pH 7.4) and 95 μL of human plasma to a final concentration 2.5 mM. After incubation for the indicated time, proteins were denatured by the addition of ACN, and samples were centrifuged to collect the clear supernatant and stored at -30 °C until analysis; for releasing analysis, synthesized conjugates were dissolved in DMSO, and the analysis solutions were prepared by diluting 50 μL of stock in 750 μL of PBS (pH 7.4, containing 5 μM, 1 mM, or 5 mM GSH) to a final concentration 2.5 mM. After incubation for the indicated time, samples were centrifuged to collect the clear supernatant and stored at -30 °C until analysis. RP-HPLC injections were carried out under the specified conditions, and the area of peak was integrated for further calculation.

Statistical Analysis. All data were obtained at least in triplicate, and results are reported as mean ± mean of standard deviation (S.E.M.). Comparisons among groups were analyzed via *t* tests, one-way ANOVA, and two-way ANOVA analysis using SAS Version 9.2 (SAS Institute, Cary, NC). The statistical significance was determined: n.s., nonsignificant difference; *****P* < 0.0001; **P* < 0.05.

■ ASSOCIATED CONTENT

Supporting Information

The Supporting Information is available free of charge at <https://pubs.acs.org/doi/10.1021/acs.jmedchem.0c00897>.

Synthesis of linkers **14** and **19**, NMR spectra of all new structures, and ¹H NMR and ¹³C NMR spectra of compounds; serum stability of compounds **5** and **9** and HPLC purities of final compounds; Western analysis of CRC and NHDF cell lines; and detailed UPLC-MS/MS analyses to quantify serum and organ concentrations of 5-FU and compound **7** (PDF)

Molecular formula strings (CSV)

■ AUTHOR INFORMATION

Corresponding Author

Pi-Hui Liang – School of Pharmacy, College of Medicine, National Taiwan University, Taipei 100, Taiwan; The Genomics Research Center, Academia Sinica, Taipei 128, Taiwan; orcid.org/0000-0001-6668-4642; Email: phliang@ntu.edu.tw

Authors

Chun-Kai Chang – School of Pharmacy, College of Medicine, National Taiwan University, Taipei 100, Taiwan

Pei-Fang Chiu – School of Pharmacy, College of Medicine, National Taiwan University, Taipei 100, Taiwan

Hui-Yi Yang – School of Pharmacy, College of Medicine, National Taiwan University, Taipei 100, Taiwan

Yu-Pu Juang – School of Pharmacy, College of Medicine, National Taiwan University, Taipei 100, Taiwan

Yen-Hsun Lai – School of Pharmacy, College of Medicine, National Taiwan University, Taipei 100, Taiwan

Tzung-Sheng Lin – School of Pharmacy, College of Medicine, National Taiwan University, Taipei 100, Taiwan

Lih-Ching Hsu – School of Pharmacy, College of Medicine, National Taiwan University, Taipei 100, Taiwan

Linda Chia-Hui Yu – Graduate Institute of Physiology, College of Medicine, National Taiwan University, Taipei 100, Taiwan

Complete contact information is available at:

<https://pubs.acs.org/10.1021/acs.jmedchem.0c00897>

Author Contributions

P.-H.L. designed the research, and C.-K.C., H.-Y.Y., P.-F.C., and Y.-H.L. synthesized the compounds. C.-K.C. performed *in vitro* cytotoxicity assay and *in vivo* assay. C.-K.C., H.-Y.Y., and T.-S.L. did the stability assay. P.-F.C. and Y.-P.J. performed western analysis. L.-C.H. performed GLUT1 inhibition assay and provided NHDF cells. L.C.-H.Y. provided HT-29 and HCT-11 cell lines and designed animal experiments. C.-K.C. and P.-H.L. wrote the manuscript, which was contributed by all authors, who have approved the submitted version of the manuscript.

Funding

This research was financially supported by the Ministry of Science and Technology (MOST 108-3114-Y-001-002; 107-2320-B-002-019-MY3; 106-2320-B-002-017; and 104-2320-B-002-008-MY3) and Academia Sinica [grant no. AS-SUMMIT-109].

Notes

The authors declare no competing financial interest.

■ ACKNOWLEDGMENTS

C.-K.C. and P.-F.C. are supported by a scholarship from the XinChen Medical Research Foundation, Taiwan. Y.-P.J. is supported by the Program of Research Performance Enhancement via Students Entering Ph.D. Programs Straight from an Undergraduate/Master's Program from National Taiwan University.

■ ABBREVIATIONS

ACN, acetonitrile; AOM, azoxymethane; CRC, colorectal cancer; DCC, dicyclohexylcarbodiimide; DCM, dichloromethane; DMAP, 4-dimethylaminopyridine; DMEM, Dulbecco's Modified Eagle Medium; DMF, dimethylformamide; DPD, dihydropyrimidine dehydrogenase; DSS, dextran sulfate sodium; 5-FU, 5-fluorouracil; GLUT, glucose transporter; GSH, glutathione; Hex, hexane; HRMS, high-resolution mass spectrometry; i.v., intravenous; i.p., intraperitoneal; KRB, Krebs Ringer bicarbonate buffer; 2-NBDG, (2-N-(7-nitrobenz-2-oxa-1,3-diazol-4-yl)amino)-2-deoxy-D-glucose; NHDF, normal human dermal fibroblasts; NMR, nuclear magnetic resonance; PBS, phosphate buffered saline; PK, pharmacokinetic; RP-HPLC, reversed phase high-performance liquid chromatography; SGLT, sodium-glucose cotransporters; SMDC, small molecule drug conjugation; SRB, sulforhodamine B; TBTA, tris(1-benzyl-1H-1,2,3-triazol)-4-yl phosphine; TCEP, tris(2-carboxyethyl)phosphine; THF, tetrahydrofuran

REFERENCES

- (1) Bray, F.; Ferlay, J.; Soerjomataram, I.; Siegel, R. L.; Torre, L. A.; Jemal, A. Global cancer statistics 2018: GLOBOCAN estimates of incidence and mortality worldwide for 36 cancers in 185 countries. *CA: Cancer J. Clin.* **2018**, *68*, 394–424.
- (2) Loupakis, F.; Cremolini, C.; Masi, G.; Lonardi, S.; Zagonel, V.; Salvatore, L.; Cortesi, E.; Tomasello, G.; Ronzoni, M.; Spadi, R.; Zaniboni, A.; Tonini, G.; Buonadonna, A.; Amoroso, D.; Chiara, S.; Carlomagno, C.; Boni, C.; Allegrini, G.; Boni, L.; Falcone, A. Initial therapy with FOLFOXIRI and bevacizumab for metastatic colorectal cancer. *N. Engl. J. Med.* **2014**, *371*, 1609–1618.
- (3) Boige, V.; Mendiboure, J.; Pignon, J. P.; Loriot, M. A.; Castaing, M.; Barrois, M.; Malka, D.; Trégouët, D. A.; Bouché, O.; Le Corre, D.; Miran, I.; Mulot, C.; Ducreux, M.; Beaune, P.; Laurent-Puig, P. Pharmacogenetic assessment of toxicity and outcome in patients with metastatic colorectal cancer treated with LV5FU2, FOLFOX, and FOLFIRI: FFC2 2000-05. *J. Clin. Oncol.* **2010**, *28*, 2556–2564.
- (4) Modest, D. P.; Pant, S.; Sartore-Bianchi, A. Treatment sequencing in metastatic colorectal cancer. *Eur. J. Cancer* **2019**, *109*, 70–83.
- (5) Munker, S.; Gerken, M.; Fest, P.; Ott, C.; Schnoy, E.; Fichtner-Feigl, S.; Wiggermann, P.; Vogelhuber, M.; Herr, W.; Stroszczyński, C.; Schlitt, H. J.; Evert, M.; Reng, M.; Klinkhammer-Schalke, M.; Teufel, A. Chemotherapy for metastatic colon cancer: No effect on survival when the dose is reduced due to side effects. *BMC Cancer* **2018**, *18*, 455.
- (6) Cuezva, J. M.; Krajewska, M.; de Heredia, M. L.; Krajewski, S.; Santamaria, G.; Kim, H.; Zapata, J. M.; Marusawa, H.; Chamorro, M.; Reed, J. C. The bioenergetic signature of cancer: a marker of tumor progression. *Cancer Res.* **2002**, *62*, 6674–6681.
- (7) Medina, R. A.; Owen, G. I. Glucose transporters: expression, regulation and cancer. *Biol. Res.* **2002**, *35*, 9–26.
- (8) Bhattacharya, B.; Mohd Omar, M. F.; Soong, R. The Warburg effect and drug resistance. *Br. J. Pharmacol.* **2016**, *173*, 970–979.
- (9) Guo, G. F.; Cai, Y. C.; Zhang, B.; Xu, R. H.; Qiu, H. J.; Xia, L. P.; Jiang, W. Q.; Hu, P. L.; Chen, X. X.; Zhou, F. F.; Wang, F. Overexpression of SGLT1 and EGFR in colorectal cancer showing a correlation with the prognosis. *Med. Oncol.* **2011**, 197–203.
- (10) Wright, E. M.; Loo, D. D. F.; Hirayama, B. A. Biology of human sodium glucose transporters. *Physiol. Rev.* **2011**, *91*, 733–794.
- (11) Villani, L. A.; Smith, B. K.; Marcinko, K.; Ford, R. J.; Broadfield, L. A.; Green, A. E.; Houde, V. P.; Muti, P.; Tsakiridis, T.; Steinberg, G. R. The diabetes medication Canagliflozin reduces cancer cell proliferation by inhibiting mitochondrial complex-I supported respiration. *Mol. Metab.* **2016**, *5*, 1048–1056.
- (12) Younes, M.; Lechago, L. V.; Somoano, J. R.; Mosharaf, M.; Lechago, J. Wide expression of the human erythrocyte glucose transporter Glut1 in human cancers. *Cancer Res.* **1996**, *56*, 1164–1167.
- (13) Haber, R. S.; Rathan, A.; Weiser, K. R.; Pritsker, A.; Itzkowitz, S. H.; Bodian, C.; Slater, G.; Weiss, A.; Burstein, D. E. GLUT1 glucose transporter expression in colorectal carcinoma: a marker for poor prognosis. *Cancer* **1998**, *83*, 34–40.
- (14) Brown, R. S.; Wahl, R. L. Overexpression of Glut-1 glucose transporter in human breast cancer An immunohistochemical study. *Cancer* **1993**, *72*, 2979–2985.
- (15) Law, A. A.; Collie-Duguid, E. S.; Smith, T. A. Influence of resistance to 5-fluorouracil and tomudex on [¹⁸F]FDG incorporation, glucose transport and hexokinase activity. *Int. J. Oncol.* **2012**, *41*, 378–382.
- (16) Ma, Y.-S.; Yang, I.-P.; Tsai, H.-L.; Huang, C.-W.; Juo, S.-H. H.; Wang, J.-Y. High glucose modulates antiproliferative effect and cytotoxicity of 5-fluorouracil in human colon cancer cells. *DNA Cell Biol.* **2014**, *33*, 64–72.
- (17) Huang, C.-Y.; Huang, C.-Y.; Pai, Y.-C.; Lin, B.-R.; Lee, T.-C.; Liang, P.-H.; Yu, L.-C. Glucose metabolites exert opposing roles in tumor chemoresistance. *Front. Oncol.* **2019**, *9*, 1282.
- (18) Ma, P.; Chen, J.; Bi, X.; Li, Z.; Gao, X.; Li, H.; Zhu, H.; Huang, Y.; Qi, J.; Zhang, Y. Overcoming multidrug resistance through the GLUT1-mediated and enzyme-triggered mitochondrial targeting conjugate with redox-sensitive Paclitaxel release. *ACS Appl. Mater. Interfaces* **2018**, *10*, 12351–12363.
- (19) Shi, Y.; Liu, S.; Ahmad, S.; Gao, Q. Targeting key transporters in tumor glycolysis as a novel anticancer strategy. *Curr. Top. Med. Chem.* **2018**, *18*, 454–466.
- (20) Shao, X.; Bai, N.; He, K.; Ho, C. T.; Yang, C. S.; Sang, S. Apple polyphenols, phloretin and phloridzin: new trapping agents of reactive dicarbonyl species. *Chem. Res. Toxicol.* **2008**, *21*, 2042–2050.
- (21) Cao, X.; Fang, L.; Gibbs, S.; Huang, Y.; Dai, Z.; Wen, P.; Zheng, X.; Sadee, W.; Sun, D. Glucose uptake inhibitor sensitizes cancer cells to daunorubicin and overcomes drug resistance in hypoxia. *Cancer Chemother. Pharmacol.* **2007**, *59*, 495–505.
- (22) Chang, H. C.; Yang, S. F.; Huang, C. C.; Lin, T. S.; Liang, P. H.; Lin, C. J.; Hsu, L. C. Development of a novel non-radioactive cell-based method for the screening of SGLT1 and SGLT2 inhibitors using 1-NBDG. *Mol. Biosyst.* **2013**, *9*, 2010–2020.
- (23) Abdel-Wahab, A. F.; Mahmoud, W.; Al-Harizy, R. M. Targeting glucose metabolism to suppress cancer progression: prospective of anti-glycolytic cancer therapy. *Pharmacol. Res.* **2019**, *150*, 104511.
- (24) Scafoglio, C.; Hirayama, B. A.; Kepe, V.; Liu, J.; Ghezzi, C.; Satyamurthy, N.; Moatamed, N. A.; Huang, J.; Koepsell, H.; Barrio, J. R.; Wright, E. M. Functional expression of sodium-glucose transporters in cancer. *Proc. Natl. Acad. Sci. U. S. A.* **2015**, *112*, E4111–E4119.
- (25) Pessin, J. E.; Bell, G. I. Mammalian facilitative glucose transporter family: structure and molecular regulation. *Annu. Rev. Physiol.* **1992**, *54*, 911–930.
- (26) Huang, C. Y.; Yu, L. C. Distinct patterns of interleukin-12/23 and tumor necrosis factor alpha synthesis by activated macrophages are modulated by glucose and colon cancer metabolites. *Chin. J. Physiol.* **2020**, *63*, 7–14.
- (27) Huang, C.-Y.; Kuo, W.-T.; Huang, C.-Y.; Lee, T.-C.; Chen, C.-T.; Peng, W.-H.; Lu, K.-S.; Yang, C.-Y.; Yu, L. C.-H. Distinct cytoprotective roles of pyruvate and ATP by glucose metabolism on epithelial necroptosis and crypt proliferation in ischaemic gut. *J. Physiol.* **2017**, *595*, 505–521.
- (28) Srinivasarao, M.; Low, P. S. Ligand-targeted drug delivery. *Chem. Rev.* **2017**, *117*, 12133–12164.
- (29) Srinivasarao, M.; Galliford, C. V.; Low, P. S. Principles in the design of ligand-targeted cancer therapeutics and imaging agents. *Nat. Rev. Drug Discovery* **2015**, *14*, 203–219.
- (30) Bansal, A.; Simon, M. C. Glutathione metabolism in cancer progression and treatment resistance. *J. Cell Biol.* **2018**, *217*, 2291–2298.
- (31) Zhao, M.; Liu, Q.; Gong, Y.; Xu, X.; Zhang, C.; Liu, X.; Zhang, C.; Guo, H.; Zhang, X.; Gong, Y.; Shao, C. GSH-dependent antioxidant defense contributes to the acclimation of colon cancer cells to acidic microenvironment. *Cell Cycle* **2016**, *15*, 1125–1133.
- (32) Forman, H. J.; Zhang, H.; Rinna, A. Glutathione: overview of its protective roles, measurement, and biosynthesis. *Mol. Aspects Med.* **2009**, *30*, 1–12.
- (33) Fishkin, N.; Maloney, E. K.; Chari, R. V. J.; Singh, R. A novel pathway for maytansinoid release from thioether linked antibody–drug conjugates (ADCs) under oxidative conditions. *Chem. Commun.* **2011**, *47*, 10752–10754.
- (34) Pan, X.; Wang, C.; Wang, F.; Li, P.; Hu, Z.; Shan, Y.; Zhang, J. Development of 5-Fluorouracil derivatives as anticancer agents. *Curr. Med. Chem.* **2011**, *18*, 4538–4556.
- (35) Ponte, J. F.; Sun, X.; Yoder, N. C.; Fishkin, N.; Laleau, R.; Coccia, J.; Lanieri, L.; Bogalhas, M.; Wang, L.; Wilhelm, S.; Widdison, W.; Pinkas, J.; Keating, T. A.; Chari, R.; Erickson, H. K.; Lambert, J. M. Understanding how the stability of the thiol-maleimide linkage impacts the pharmacokinetics of lysine-linked antibody-maytansinoid conjugates. *Bioconjugate Chem.* **2016**, *27*, 1588–1598.
- (36) Michelet, F.; Gueguen, R.; Leroy, P.; Wellman, M.; Nicolas, A.; Siest, G. Blood and plasma glutathione measured in healthy subjects by HPLC: relation to sex, aging, biological variables, and life habits. *Clin. Chem.* **1995**, *41*, 1509–1517.
- (37) Salas-Burgos, A.; Iserovich, P.; Zuniga, F.; Vera, J. C.; Fischbarg, J. Predicting the three-dimensional structure of the human facilitative glucose transporter glut1 by a novel evolutionary homology strategy: insights on the molecular mechanism of substrate migration, and

binding sites for glucose and inhibitory molecules. *Biophys. J.* **2004**, *87*, 2990–2999.

(38) Iwamoto, M.; Kawada, K.; Nakamoto, Y.; Itatani, Y.; Inamoto, S.; Toda, K.; Kimura, H.; Sasazuki, T.; Shirasawa, S.; Okuyama, H.; Inoue, M.; Hasegawa, S.; Togashi, K.; Sakai, Y. Regulation of 18F-FDG accumulation in colorectal cancer cells with mutated KRAS. *J. Nucl. Med.* **2014**, *55*, 2038–2044.

(39) Kuo, W.-T.; Lee, T.-C.; Yu, L. C.-H. Eritoran suppresses colon cancer by altering a functional balance in Toll-like receptors that bind lipopolysaccharide. *Cancer Res.* **2016**, *76*, 4684–4695.

(40) Juang, Y. P.; Lin, Y. Y.; Chan, S. H.; Chang, C. K.; Shie, J. J.; Hsieh, Y. S. Y.; Guh, J. H.; Liang, P. H. Synthesis, distribution analysis and mechanism studies of N-acyl glucosamine-bearing oleanolic saponins. *Bioorg. Chem.* **2020**, *99*, 103835.

(41) Pei, Q.; Hu, X.; Li, Z.; Xie, Z.; Jing, X. Small molecular nanomedicines made from a camptothecin dimer containing a disulfide bond. *RSC Adv.* **2015**, *5*, 81499–81501.

(42) Kuo, W.-T.; Lee, T.-C.; Yang, H.-Y.; Chen, C.-Y.; Au, Y.-C.; Lu, Y.-Z.; Wu, L.-L.; Wei, S.-C.; Ni, Y.-H.; Lin, B.-R.; Chen, Y.; Tsai, Y.-H.; Kung, J. T.; Sheu, F.; Lin, L.-W.; Yu, L. C.-H. LPS receptor subunits have antagonistic roles in epithelial apoptosis and colonic carcinogenesis. *Cell Death Differ.* **2015**, *22*, 1590–1604.

(43) Kasahara, T.; Kasahara, M. Characterization of rat Glut4 glucose transporter expressed in the yeast *Saccharomyces cerevisiae*: comparison with Glut1 glucose transporter. *Biochim. Biophys. Acta* **1997**, *1324*, 111–119.

(44) Augustin, R. The protein family of glucose transport facilitators: It's not only about glucose after all. *IUBMB Life* **2010**, *62*, 315–333.

(45) Rudakova, E. V.; Boltneva, N. P.; Makhava, G. F. Comparative analysis of esterase activities of human, mouse, and rat blood. *Bull. Exp. Biol. Med.* **2011**, *152*, 73–75.

(46) Dougherty, P. G.; Karpurapu, M.; Koley, A.; Lukowski, J. K.; Qian, Z.; Srinivas Nirujogi, T.; Rusu, L.; Chung, S.; Hummon, A. B.; Li, H. W.; Christman, J. W.; Pei, D. A peptidyl inhibitor that blocks calcineurin-NFAT interaction and prevents acute lung injury. *J. Med. Chem.* **2020**, *63*, 12853–12872.

(47) Geary, R. S.; Norris, D.; Yu, R.; Bennett, C. F. Pharmacokinetics, biodistribution and cell uptake of antisense oligonucleotides. *Adv. Drug Delivery Rev.* **2015**, *87*, 46–51.

(48) Visser, G. W. M.; Gorree, G. C. M.; Peters, G. J.; Herscheid, J. D. M. Tissue distribution of [18F]-5-fluorouracil in mice: effects of route of administration, strain, tumour and dose. *Cancer Chemother. Pharmacol.* **1990**, *26*, 205–209.